

RESEARCH

An SDR Implementation of WiFi Receiver for Mitigating Multiple Co-Channel ZigBee Interferers

Sumit Kumar^{1*}, Florian Kaltenberger¹, Alejandro Ramirez² and Bernhard Kloiber²

Abstract

Machine-to-Machine (M2M) communication is one of the vertical sectors that will benefit from 5G communication systems, but today these systems are still dominated by technologies such as ZigBee and WiFi. An M2M scenario will experience dense deployment of ZigBee and WiFi nodes in order to route the data from one end to the other. In the 2.4 GHz ISM band, both the technologies perform co-channel overlapped operation and hence face severe cross technology co-channel interference (CCI). In contrast to cellular systems, which solves the CCI by centralized coordination through the base station, addressing CCI in ISM band is non-trivial due to heterogeneous wireless technologies and lack of centralized coordination. In this work, we first present interference mitigating receiver architectures for OFDM based WiFi using single and multiple antennas. Our single antenna work is based on the localized estimation of excess noise caused by single and multiple co-channel narrowband interferers and scaling the Log Likelihood Ratios (LLRs) of affected WiFi subcarriers. The simulation shows our method achieves a significant gain in SNR compared to the conventional method for a given Packet Error Rate (PER) criterion. Next, we discuss Maximal Ratio Combiner with LLR scaling (MLSC), which is a multi-antenna extension to our previous work. The simulation shows MLSC achieves diversity gain apart from the gain in SNR. Further, we propose Soft Bit Maximal Ratio Combiner with LLR Scaling (SB-MLSC). SB-MLSC is an easy to implement version of MLSC. However, diversity combining in SB-MLSC is performed by combining the LLRs. Nonetheless, simulations show equivalence in performance by SB-MLSC and MLSC. Finally, as a significant part of this work, we implemented all our methods using Software Defined Radio (SDR) and performed over-the-air (OTA) testing in the 2.4 GHz ISM band using standard WiFi and ZigBee frames. Results of OTA tests fall in complete agreement with our simulations indicating the practical applicability of our methods. Our methods apply to all the standards which are based on OFDM and face narrowband co-channel interference. Additionally, since our work focuses only on receiver side modifications, they can be integrated with the existing infrastructure with minimal modifications.

Keywords: Co-Channel Interference; WiFi-ZigBee; Interference Mitigation; Software Defined Radio

1 Introduction

The rapid increase in low cost heterogeneous wireless devices and inherent limitation of Radio-Frequency (RF) spectrum is causing Cross technology Co-Channel Interference (CT-CCI). Effects of CT-CCI are prevalent in the unlicensed Industrial Scientific Medical (ISM) bands which lack centralized control over devices operating on heterogeneous standards. This is in contrast to the cellular standards operating in li-

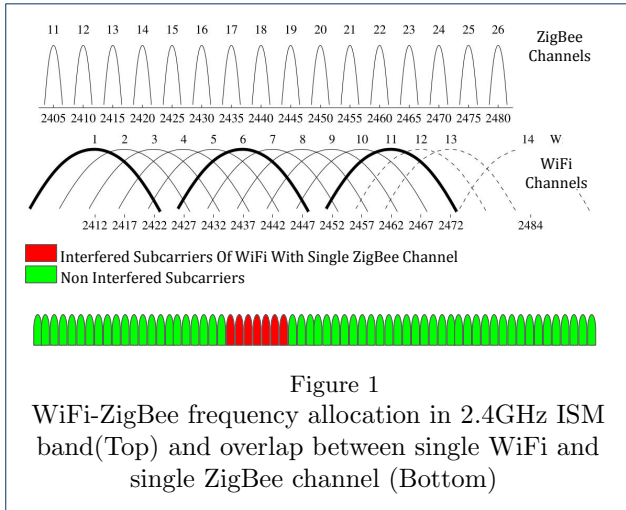
censed frequency bands where CCI^[1] is caused due to homogeneous wireless standards and effectively mitigated by a centralized control of transmit time and transmit power. However, in the Industrial, Scientific and Medical (ISM) bands where heterogeneous wireless standards operate on overlapped frequency bands, application of methods used in cellular communication to mitigate CCI is not trivial. Reason being lack of centralized control and disparity in physical layer implementations of the wireless standards.

In this work, our application scenarios are smart homes and modern automated factories where there

^[1]In cellular networks, as the standards are homogeneous, there is only CCI not CT-CCI

*Correspondence: sumit.kumar@eurecom.fr

¹Communication Systems, Eurecom, Sophia Antipolis, Biot, France
Full list of author information is available at the end of the article



is dense deployment of wireless sensors and Machine-to-Machine communications plays key role in routing the sensory data to the processing centers. These wireless sensors predominantly use Wireless Local Area Networks (WLAN; based on IEEE 802.11) such as IEEE 802.11 a/b/g/n/ah, and Wireless Personal Area Networks (WPAN) such as IEEE 802.15.4 and IEEE 802.15.1. Our frequency of interest is 2.4 GHz ISM band which has a usable bandwidth of 80 MHz and being shared by several heterogeneous wireless standards such as IEEE 802.11a/b/g and IEEE 802.15.4, IEEE 802.15.1 etc. Among them, our standards of interest are OFDM based wideband IEEE 802.11g (popularly known as WiFi) and narrowband ZigBee which uses physical layer of IEEE 802.15.4.

Previous simulations and field trials [1][2] have shown that even though both WiFi and ZigBee posses Carrier Sense Multiple Access with Collision Avoidance (CSMA/CA) [3][1], both of them suffer significant throughput degradation. Main reasons behind collisions are hidden and blind terminals where the formation of hidden and blind terminals could be as high as 41% in a randomly deployed network [4] [5]. The extent of degradation depends on received power levels (RXP) and the degree of time/frequency overlap of the interfering signals.

1.1 WiFi ZigBee Co-Channel Interference in Frequency Domain

IEEE 802.11g (WiFi) operating in 2.4 GHz band is an OFDM based wideband system. We have not chosen IEEE 802.11n because we propose methods for OFDM based WiFi receivers; hence, methods developed for IEEE 802.11g are also applicable to IEEE 802.11n. It is 20MHz wide and divided into 64 orthogonal subcarriers, each 312.5 kHz wide. In contrast, ZigBee operating in 2.4 GHz is a narrowband system

with a bandwidth of 2 MHz and uses O-QPSK (Offset-Quadrature Phase Shift Keying) and DSSS (Direct Sequence Spread Spectrum) in its physical layer. Figure 1 shows within every orthogonal channel (20 MHz each) of WiFi, i.e., 2.412, 2.437, 2.462 GHz, 4 ZigBee channels (2 MHz each) completely overlap. As discussed previously, both WiFi and ZigBee apply CSMA/CA as collision avoidance mechanism, but still, the collision happens due to the hidden and blind terminals. and differences in channel sensing/response time [6].

Although most of the past studies indicate that WiFi is the culprit for interference and ZigBee as the victim, which is true in the majority of the situations [7][8][9]. Reason being higher transmit power of WiFi compared to ZigBee. However, in the event of a collision, Packet Error Rate(PER) of WiFi significantly increases [10][11]; especially when there is a WiFi receiver in the immediate proximity of a ZigBee transmitter. To verify the PER degradation of WiFi, we simulated a scenario of interference between a single antenna WiFi receiver and a single antenna ZigBee transmitter in the absence of CSMA/CA [2]. Plots of simulation, as shown in Figure 2, indicate severe degradation of WiFi PER for all the Modulation and Coding Scheme (MCS) which agree with the previous works.

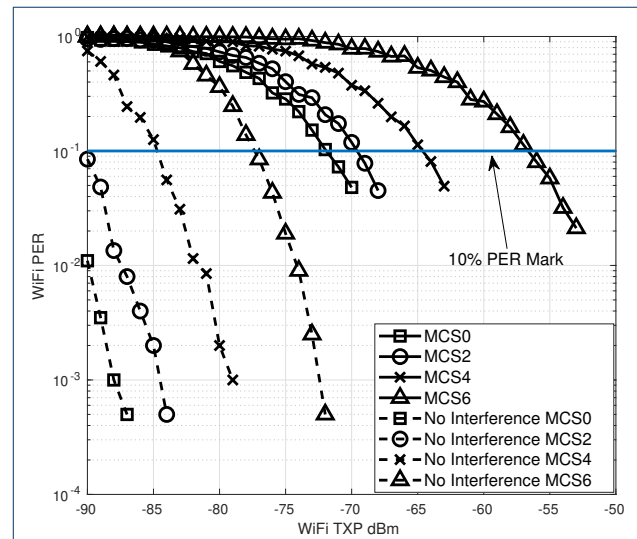


Figure 2

PER of single antenna WiFi receiver in the presence and absence of single antenna ZigBee transmitter(transmit power -85 dBm). For all WiFi MCS, we observe severe PER degradation.

Recognizing that WiFi can also be a victim of CCI caused by ZigBee, in this work, we address the issue of

[2] Table 1 contains simulation parameters for this figure.

CCI faced by WiFi nodes in the 2.4 GHz ISM band due to dense deployment of ZigBee nodes. In other words, IEEE 802.11g (WiFi) is our desired signal and IEEE 802.15.4 (ZigBee) is the co-channel interferer.

1.2 Related Work

1.2.1 Single-antenna Techniques

Among single antenna interference mitigation techniques, Successive Interference Cancellation (SIC) [12] is one of the most effective methods. The Signal-to-Interference (SIR) difference between WiFi and ZigBee is around 5 – 20 dB which is suitable for SIC [7]. In [3], authors propose a decision-directed channel estimation along with soft Viterbi decoder for WiFi followed by Successive Interference Cancellation (SIC) which results in throughput gain for both WiFi and ZigBee. However such difference of power between WiFi and ZigBee is not always guaranteed especially when the ZigBee transmitter is situated very near to the WiFi receiver. In our previous work [10], we proposed methods to assist the SIC procedure in a single antenna WiFi receiver which helps in improving the PER of WiFi facing interference from multiple co-channel narrowband ZigBee interferers. Our work is based on the localized estimation of excess noise caused by narrowband interferers and scaling the affected Log Likelihood Ratios of OFDM subcarriers. Authors in [13] benefit from known preambles of WiFi during SIC, which proves to be very effective; however, the method is limited to WiFi-to-WiFi interference and does not address cross-technology interference. In [14], authors propose a data-dependent model of ZigBee along with modifications to the MAC layer to increase the throughput of ZigBee. However, any modification to the MAC layer requires additional changes in the existing standard. Similarly, authors in [7] and [15] propose to send fake preambles and jamming signals to make ZigBee more visible to WiFi and force WiFi to back-off during channel contention. However anti-jamming capabilities of WiFi can make such solutions infeasible [16]. In our work, we exclusively focus only on such methods which propose modifications only on the receiver side. Any proposed modification on the transmitter side requires changing the standard and hence, making the modifications challenging to integrate into the existing infrastructure.

1.2.2 Multi-antenna Techniques

Multi-antenna interference mitigation methods are dominated by beamforming. Some of the notable works include [17] and [18]. Authors in [17] propose chain decoding of mutually interfering WiFi signals and modifications in MAC layer. Despite being effective, it requires changes in the WiFi standard and is limited

to CCI between WiFi only. Authors in [18] propose to precode the interfering signals on the transmitter side which again requires to change the WiFi standard. However, such solutions are difficult to integrate into existing infrastructures. Authors in [19] propose a non-beamforming approach for multi-antenna OFDM receivers where SINR based Maximal Ratio Combining is performed, however, the accuracy of their solution depends on averaging over multiple OFDM symbols. Authors in [20], estimate noise variance per subcarrier to mitigate the colored nature of inter-carrier-interference in OFDM systems. However, they don't use Soft Decision Viterbi Decoder (SDVD) and hence fail to utilize channel state information during channel decoding. Performance of SDVD along with channel state information is significantly better than Hard Decision Viterbi Decoder (HDVD) in an interference limited environment [21]. Authors in [22] propose technology independent MIMO (TIMO) to utilize channel estimate ratio of interferers on the different antenna of the receiver, but TIMO fails to utilize the easily available diversity gain [11]. An old yet effective method to mitigate interference in multi-antenna systems is Optimal Combiner (OC) [23] however, OC requires computation of Interference-Plus-Noise (IPN) matrix. As the number of antennas grows, computation of IPN becomes prohibitively high due to matrix inversion of the order of $N \times N$ where N is the number of receiver antennas. In an extension to our previous work of single antenna WiFi receiver, we further proposed Maximal Ratio Combiner with LLR Scaling (MLSC) in [11]. MLSC not only helps in mitigating narrowband interferers but also provides diversity gain to a multi-antenna WiFi receiver. Simulations showed MLSC performing equivalent to Optimal Combiner [23] and significantly better than TIMO. Additionally in [11] we proposed Diversity Combining TIMO (DC-TIMO), a modification to existing TIMO. DC-TIMO is capable of interference nulling as well as benefits from diversity gain.

1.2.3 Interference Detection

In addition to interference mitigation, immediate detection and positioning of interferer (center frequency) is an essential step to be performed before performing any interference mitigation/cancellation scheme at the receiver. Unfortunately, interference detection and positioning have not been researched widely at the physical layer (PHY) in ISM bands for unmanaged networks. In [24], authors proposed a method to detect ZigBee interference on WiFi by analyzing packet error rate (PER) at the MAC layer. Authors of [25] take a similar approach where ZigBee interference to WiFi networks is detected by PER analysis. In [22], authors

proposed to detect interference by monitoring soft bit errors in OFDM. However, PER and soft bit error could even occur due to severe fading. As a byproduct of our work in [10], we proposed a method of quick detection of multiple narrowband interferers using WiFi preambles. The method proved to be effective even in the presence of very low powered co-channel interference.

1.3 Contributions

Interference mitigation in unmanaged networks is still a challenging problem. In continuation to our previous works on interference mitigation for single antenna WiFi receivers [10] and multi-antenna WiFi receivers [11], in this work, we have primarily focused on their applicability in real-time by implementing them using Software Defined Radio (SDR). Our main contributions in this work are summarized as follows:

- 1 We propose Soft Bit Maximal Ratio Combiner with LLR Scaling (SB-MLSC) for mitigating narrowband interference in a multi-antenna WiFi receiver. SB-MLSC performs equivalently to MLSC; however, it is easy to prototype SB-MLSC in the existing SDR software packages.
- 2 We implemented our single antenna contribution [10] using Ettus Universal Software Radio Peripheral (USRP) [26] and a combination of GNU Radio [27] and Openairinterface [28] SDR software packages. Further, we performed over-the-air (OTA) testing of our methods against standard compliant WiFi (IEEE 802.11g) frames being interfered by standard compliant ZigBee (IEEE 802.15.4) frames [3].
- 3 We implemented our dual-antenna interference mitigation method for WiFi, i.e., SB-MLSC using USRP and a combination of GNU Radio and Openairinterface followed by OTA testing against standard compliant WiFi and ZigBee frames.

Results of the OTA tests fall in close agreement with our simulation results showing the practical applicability of our proposed methods. All our proposed methods for WiFi are also applicable to wideband OFDM based systems which face co-channel narrowband interference. Additionally, the proposed signal processing methods and hardware implementations require modifications only on the receiver side and hence can be integrated into the existing infrastructure with minimal modifications.

[3] We took the binary dump of WiFi and ZigBee frames generated by MATLAB and transmitted them using USRP SDR. The frames were detected by commercial WiFi and ZigBee nodes which established the standard compliance of the WiFi and ZigBee frames generated by MATLAB toolboxes

1.4 Organization

Section 2 discusses the necessary background and details of narrowband interference mitigating receiver architectures for WiFi which is based on our previous works on single and multi-antenna WiFi receivers. Details of the proposed method in this work are presented in Section 3. Section 4 presents the simulations of proposed method and discussion on results. Section 5 details our SDR implementation and discusses over-the-air testing results. Finally Section 6 summarizes our conclusions.

2 Receiver Architectures for Narrowband Interference Mitigation

In this section, we present the details of our previous works related to interference mitigation in single and multi-antenna WiFi receivers. We provide the necessary background for understanding our proposed method which is presented in Section 3.

2.1 Interference Mitigation in Single Antenna WiFi Receivers

2.1.1 Conventional Noise Variance Estimation

We first discuss the conventional way of computing the noise variance in a WiFi frame. A typical WiFi frame consisting of OFDM data symbols is preceded by preambles known as Short Training Sequence (STS) and Long Training Sequence (LTS) [29] as shown in Figure 3. LTS consists of two identical OFDM sym-



Figure 3
WiFi Frame Structure: LTS-1 and LTS-2 are used for channel and noise variance estimation

bols which are used for channel and noise variance estimation. After N (64 for WiFi) point FFT a received WiFi sample in the frequency domain can be written as:

$$Y(i, j) = X(i, j)H(i, j) + n(i, j), \quad 1 \leq i \leq N, \quad (1)$$

where $Y(i, j)$, $X(i, j)$ are complex samples representing received and sent symbols on the i -th subcarrier of the j -th OFDM symbol, respectively. Also, $H(i, j)$ is the channel transfer function of the i -th subcarrier for the j -th OFDM symbol. Term $n(i, j)$ contains components from both thermal noise, which is Gaussian and interference, which is not necessarily Gaussian. However, for this work we model both noise and interference as Gaussian with zero mean and variance

$\sigma^2 = \mathbb{E} \{|n(i, j)|^2\}$. The same LTS is used to compute $\hat{\sigma}^2$ which is an estimate of actual noise variance σ^2 . The conventional way [30] to obtain $\hat{\sigma}^2$ is to perform an average over noise variances of all used subcarriers U_{sub} (52 for WiFi [29]) in the LTS as follows:

$$\hat{\sigma}^2 = \frac{1}{2U_{\text{sub}}} \sum_{i=1}^{U_{\text{sub}}} |Y(i, 1) - Y(i, 2)|^2, \quad (2)$$

where $Y(i, 1)$, $Y(i, 2)$ are the complex samples corresponding to i -th subcarrier of the first and second LTS symbols respectively. This $\hat{\sigma}^2$ is used as noise variance for all the subcarriers of the OFDM data symbols following the LTS, i.e., SIGNAL and Payload field of IEEE 802.11g. Such estimation of noise variance works correctly when the noise variance is flat over the entire bandwidth of the OFDM frame. However, performance degradation is observed in the presence of co-channel narrowband interferers.

2.1.2 LLR Scaling

A Soft Decision Viterbi Decoder (SDVD) requires Log Likelihood Ratios (LLR) in contrast to Hard Decision Viterbi Decoder (HDVD) which requires bit values. Approx LLR is an efficient way to compute LLR [31]. Approx LLR $\Lambda(i, j, l)$ of the l -th bit corresponding to i -th subcarrier from j -th OFDM symbol is obtained as follows [32, Eq-2]:

$$\Lambda(i, j, l) = \frac{\min_{z \in Z_0^l} (|Y(i, j) - H(i, j)z|^2)}{\hat{\sigma}^2} - \frac{\min_{z \in Z_1^l} (|Y(i, j) - H(i, j)z|^2)}{\hat{\sigma}^2} \quad (3)$$

where $Z_q^{(l)} = \{z | b_l(z) = q\}$ and b_l denotes the l -th bit in the gray mapping of z and $\hat{\sigma}^2$ is the conventional noise variance estimate. We observe that $\hat{\sigma}^2$ acts as a scaling factor which scales the LLRs $\Lambda(i, j, l)$ according to the extent of noise variance on that subcarrier.

Expression (3), in the case of AWGN, leads to scaling of Λ 's corresponding to all OFDM subcarriers by the same $\hat{\sigma}^2$ since $\hat{\sigma}^2$ does not vary significantly over the subcarriers. We term this method as Conventional LLR Scaling (**Conv-SC**) for the rest of this work. However, this is not the case in the presence of narrowband interference where noise power is higher over S_{interf} (The set of red subcarriers in Figure 1) compared to $S_{\text{non-interf}}$ (The set of green subcarriers in Figure 1). In such case, $\hat{\sigma}^2$ being the average noise variance over entire U_{sub} does not provide local noise variance (LNV) information across the subcarriers. Hence,

in the presence of narrowband interferers, local estimation of noise power over S_{interf} and $S_{\text{non-interf}}$ is required in order to justify the scaling of $\Lambda(i, j, l)$ as in (3).

In the following, we discuss our work of [10] where we propose to perform localized estimation of noise variance on S_{interf} and $S_{\text{non-interf}}$ and then use them to scale the LLRs.

2.1.3 Method-1: LNV Estimation in the presence of K Narrowband Interferers and LLR Scaling (LNV-SC)

We start with a generalized case of K single antenna uncorrelated narrowband interferers (K single antenna ZigBee transmitters) and a single antenna WiFi receiver. In our settings, S_k is the set of WiFi subcarriers affected by the k -th interferer ($k = 1, \dots, K$) and S_0 is the set of all the subcarriers unaffected by any of the k interferers such that $S_0 \cup S_1 \cup \dots \cup S_K = S_{\text{WiFi}}$. As the center frequencies of different wireless standards are fixed and their bandwidths are predefined, the knowledge of sets S_k and the set S_0 can be obtained a priori. An exemplary illustration for the case of 4 ZigBee interferers, centered at 2.430 (channel-16), 2.435 (channel-17), 2.440 (channel-18) and 2.445 (channel-19) GHz interfering a single WiFi channel centered at 2.437 GHz is shown in Figure-4 for clarity. In this case $S_1 = \{1 \dots 7\}$ and $S_2 = \{17 \dots 23\}$, $S_3 = \{32 \dots 38\}$, $S_4 = \{48 \dots 52\}$ [4], $S_0 = S_{\text{WiFi}} - S_1 - S_2 - S_3 - S_4$. Thus, $|S_1| = |S_2| = |S_3| = |S_4| = 7$, $|S_0| = 24$ and $|S_{\text{WiFi}}| = U_{\text{sub}}$ where $|B|$ denotes the cardinality of the set B .

For $k = 0, 1, \dots, K$, the LNV estimate is defined as follows:

$$\hat{\sigma}_{S_k}^2 = \frac{1}{2|S_k|} \sum_{i \in S_k} |Y(i, 1) - Y(i, 2)|^2. \quad (4)$$

We further define an index vector as

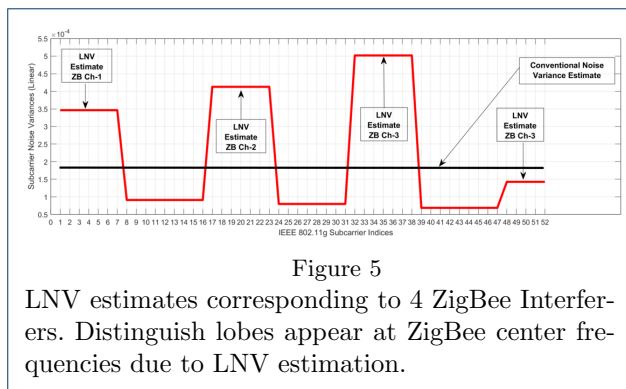
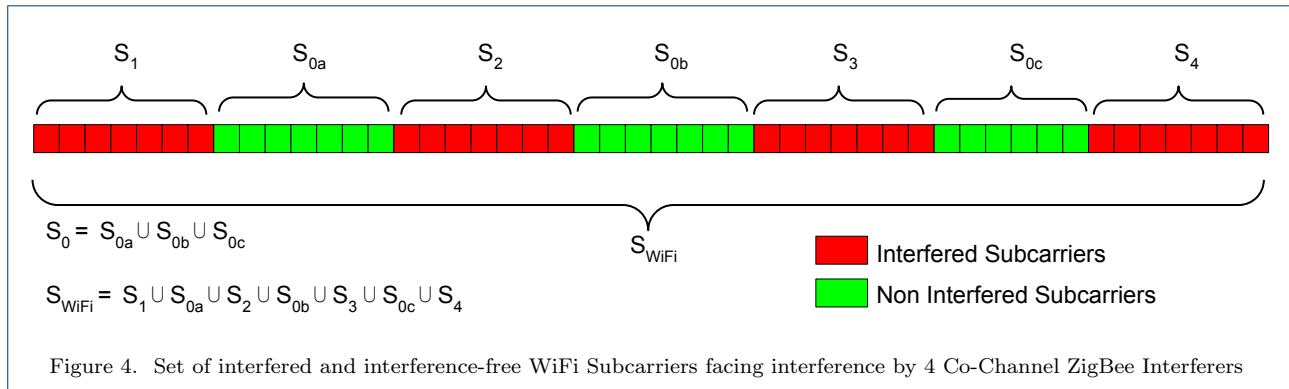
$$[\mathbf{V}_{S_k}]_i = \begin{cases} 1, & i \in S_k \\ 0, & i \notin S_k \end{cases} \quad i = 1, 2, \dots, U_{\text{sub}}. \quad (5)$$

Using (4) and (5), we define a vector of noise variances over U_{sub} as:

$$\hat{\sigma}^2 = \sum_{k=0}^K \mathbf{V}_{S_k} \hat{\sigma}_{S_k}^2, \quad (6)$$

Corresponding to Figure-4, a plot of LNV estimates, i.e., $\hat{\sigma}^2$ for 4 ZigBee interferers to a single WiFi channel is shown in Figure 5. In Figure 5 the conventionally es-

[4]The last ZigBee channel affects only 5 subcarriers within the used subcarriers. Remaining two affect subcarriers, i.e., 53 and 54 are unused



timated noise variance, i.e., $\hat{\sigma}^2$ is shown by a flat black line as it is constant over the entire span of used subcarriers. In contrast, the plot of LNV vector, i.e., $\hat{\sigma}^2$, produce distinguishably elevated lobes centered on the corresponding ZigBee center frequencies. Such lobes give information about two things: the presence of interferers and the excess noise variance induced by the interferers.

Finally using (4), (5) and (6), we can modify (3) to obtain the scaled LLRs as

$$A(i, j, l) = \frac{\min_{z \in Z_0^i} (|y(i, j) - H(i, j)z|^2)}{\hat{\sigma}_i^2} - \frac{\min_{z \in Z_1^i} (|y(i, j) - H(i, j)z|^2)}{\hat{\sigma}_i^2} \quad (7)$$

where $\hat{\sigma}_i^2$ is the i -th element of the vector $\hat{\sigma}^2$ and $i = 1, 2, \dots, U_{\text{sub}}$. We term our method of LLR scaling using LNV estimates as **LNV-SC**.

Our method to estimate LNV using LTS requires an overlap between LTS of WiFi and an ongoing ZigBee transmission. But is a fair assumption as typical frame lengths of WiFi (194 μs – 542 μs) is shorter than that of ZigBee (352 μs – 4256 μs) [7].

In the following, we discuss our method of interference detection [10] which is a by-product of LNV-SC.

2.1.4 Method-2: Interference Detection with Local Noise Variances

From Figure 5, it is observed that for K number of interferers, the vector of noise variances $\hat{\sigma}^2$ observes sharp and distinguish rise in magnitude over the regions where noise is higher, i.e., where the narrowband interferers are present compared to the regions where the narrowband interferers are absent. For a given WiFi channel, the overlapping ZigBee channels center frequencies are known a priori as shown in Figure 1. Thus the elevated portions in Figure 5 give a coarse estimate of the presence of the interferers. We combine this knowledge along with a threshold detector to pinpoint the interferers as soon as they appear. Once the interferers appear, the corresponding LNV is estimated, and the LLRs are scaled using LNV-SC. The entire operation of interference detection and LLR scaling is illustrated in Figure 6.

Our proposed method of interference detection does not add any additional signal processing complexity since it is a byproduct of LNV-SC. The key advantage of our approach is that lobes could be obtained even at very low levels of interference. However, our method is effective only when there is an overlap between LTS of WiFi and an ongoing ZigBee transmission as it uses LTS (duration 0.8 μs) to calculate $\hat{\sigma}^2$. In order to detect the appearance of ZigBee interference during an ongoing WiFi transmission, pilot subcarriers embedded under every OFDM data symbols of WiFi could be used however estimation accuracy could be affected.

In the following, we discuss our work [11] which is a multi-antenna extension to LNV-SC.

2.2 Interference Mitigation in Multi Antenna WiFi Receivers

The indoor channel, especially inside home and industries are rich in multipath [33]. With the appropriate

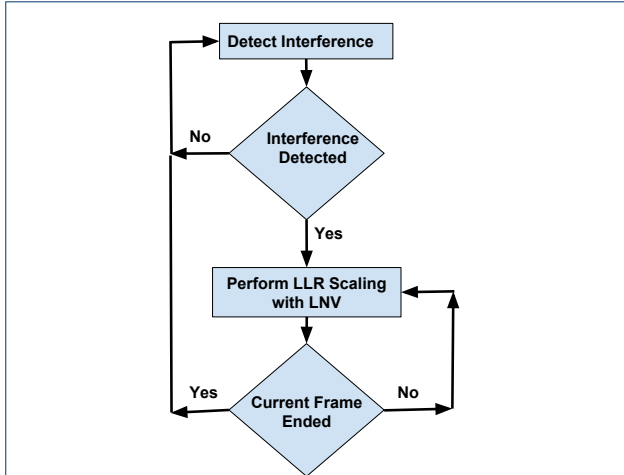


Figure 6

Flow Chart of Interference Detection and LLR Scaling. LLR scaling using LNV (LNV-SC) to be performed only during interference.

spatial separation between receiver antennas, the interference power on different antennas will be different [34]. We use this insight for applying multi-antenna diversity techniques along with our previous method of single antenna, i.e., LNV-SC. We start our development by a primer on Maximal Ratio Combining but first we establish the multi-antenna signal model.

2.2.1 Signal Model

Our signal model consists of a dual-antenna WiFi receiver (WiFi-Rx), a single antenna WiFi transmitter (WiFi-Tx), and a single antenna ZigBee transmitter (ZB-Tx) as illustrated in Figure 7. After FFT, the re-

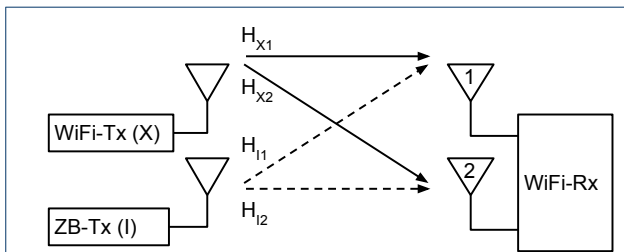


Figure 7

Signal Model: Single Antenna WiFi Transmitter, Single Antenna ZigBee Interferer and Two Antenna WiFi receiver

ceived signal vector \mathbf{Y} on i -th subcarrier of j -th WiFi OFDM symbol with the desired WiFi and interfering ZigBee samples $X(i, j)$ and $I(i, j)$ respectively can be

written as:

$$\mathbf{Y}(i, j) = X(i, j)\mathbf{H}_X(i) + I(i, j)\mathbf{H}_I(i) + \mathbf{n}(i, j), \quad (8)$$

$$\mathbf{n}(i, j) = [n_1(i, j), n_2(i, j)]^T, \quad (9)$$

$$\mathbf{H}_X(i) = [H_{X_1}(i), H_{X_2}(i)]^T, \quad (10)$$

$$\mathbf{H}_I(i) = \begin{cases} [H_{I_1}(i), H_{I_2}(i)]^T & \forall i \in S_{\text{interf}}, \\ \text{Not measured} & \forall i \in S_{\text{non-interf}}; \end{cases} \quad (11)$$

$$i = 1, 2, \dots, U_{\text{sub}}.$$

Channel estimation and all further signal processing is done in frequency domain, channels $\mathbf{H}_X(i)$ and $\mathbf{H}_I(i)$ are assumed uncorrelated, while spatial correlation ρ_X between channels of WiFi $H_{X_1}(i)$ and $H_{X_2}(i)$ and correlation ρ_I between channels of ZigBee $H_{I_1}(i)$ and $H_{I_2}(i)$ is non-zero. Note that for the interference-free WiFi subcarriers, ZigBee channels are not measured as we do not require them.

In this work, likewise (1), we also model (8) in such a way that noise contains components of interference also, as follows:

$$\mathbf{Y}(i, j) = X(i, j)\mathbf{H}_X(i) + \hat{\mathbf{n}}(i, j), \quad (12)$$

Where, entries of the noise vector $\hat{\mathbf{n}}(i, j)$ contains components from both thermal noise, which is Gaussian and interference, which is not necessarily Gaussian. However, for this work, we model both noise sources as Gaussian. The thermal noise variance is assumed to be constant for a given OFDM frame. Without loss of generality, we omit the subcarrier and OFDM symbol indexes (i, j) from notations of the received vector \mathbf{Y} , samples X and I and noise vector \mathbf{n} and use them only when required.

2.2.2 Maximal Ratio Combiner

Maximal Ratio Combiner(MRC) is one of the proven methods to increase the SNR of the signals in a multi-antenna receiver [23]. When signals come through uncorrelated paths, MRC provides diversity gain which decreases as the correlation between the paths increases. In OFDM systems, Maximal Ratio Combining (MRC) is performed on a per-subcarrier basis as follows [35]:

$$Y_{\text{MRC}} = \frac{\hat{\mathbf{H}}_X^H \mathbf{Y}}{\|\hat{\mathbf{H}}\|^2}. \quad (13)$$

Where Y_{MRC} is the complex sample after performing MRC, and $\hat{\mathbf{H}}_X$ denotes the estimated channel. However, the performance of MRC severely degrades in the presence of co-channel interference [23]. In the following, we discuss our method which overcomes this limitation of MRC by applying LNV-SC on the MRC signal.

2.2.3 Method-3: Maximal Ratio Combiner with LLR Scaling (MLSC)

We propose Maximal Ratio Combiner with LLR Scaling (MLSC) for multi-antenna WiFi receivers. An MLSC receiver performs MRC over signals from M antennas, and further scale the obtained LLRs from MRC combined signal using the vector of LNV estimates aggregated over the M antennas. This technique enables an MLSC receiver to benefit from diversity gain as well as interference mitigation simultaneously. For a M antenna WiFi receiver MLSC is performed in the following steps:

- 1 Combine the signals from all antenna branches according to MRC as in (13) and obtain Y_{MRC} .
- 2 Average the LNV vectors obtained from (6) over all the antennas as follows:

$$\hat{\sigma}_{\text{Avg}}^2 = \frac{1}{M} \sum_{m=1}^M \hat{\sigma}_m^2. \quad (14)$$

where M is the total number of antennas and $\hat{\sigma}_m^2$ is the noise variance vector corresponding to m -th antenna.

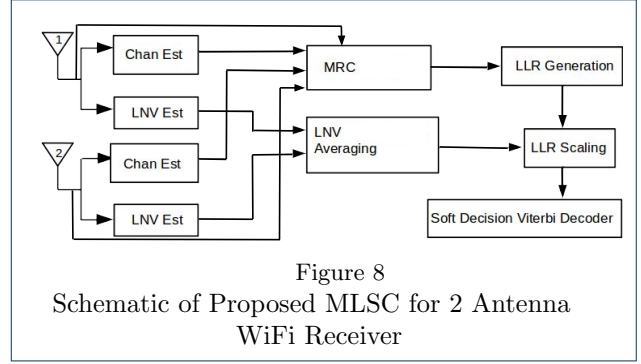
- 3 Obtain LLR corresponding to i -th subcarrier from $Y_{\text{MRC}}(i)$ and scale them using $\hat{\sigma}_{\text{Avg}}^2(i)$, which is i -th element of the vector $\hat{\sigma}_{\text{Avg}}^2$, as follows:

$$A(i, l) = \frac{\min_{z \in Z_0^l} \left(|Y_{\text{MRC}}(i) - (|H_{X_1}(i)|^2 + |H_{X_2}(i)|^2)z|^2 \right)}{\hat{\sigma}_{\text{Avg}}^2(i)} - \frac{\min_{z \in Z_1^l} \left(|Y_{\text{MRC}}(i) - (|H_{X_1}(i)|^2 + |H_{X_2}(i)|^2)z|^2 \right)}{\hat{\sigma}_{\text{Avg}}^2(i)} \quad (15)$$

For a dual antenna WiFi receiver, the schematic of MLSC is illustrated in Figure 8.

3 Proposed Method

Since our major focus in this work is to implement our interference mitigating methods using SDR and test their practical applicability, in this section we chose and analyze easy to implement alternatives of MLSC without compromising with the performance.



3.1 Soft Bit Maximal Ratio Combiner

The idea behind the usage of MRC in MLSC is to achieve diversity gain apart from interference mitigation. Conventional MRC as discussed in Section 2.2.2, is a *Symbol Level Diversity Combiner* where the bit metrics are generated after the complex samples are combined from different antenna branches. Although, simulation results in [11] showed the effectiveness of MLSC, however, a working module of MRC for WiFi is not available in GNU Radio WiFi package [36].

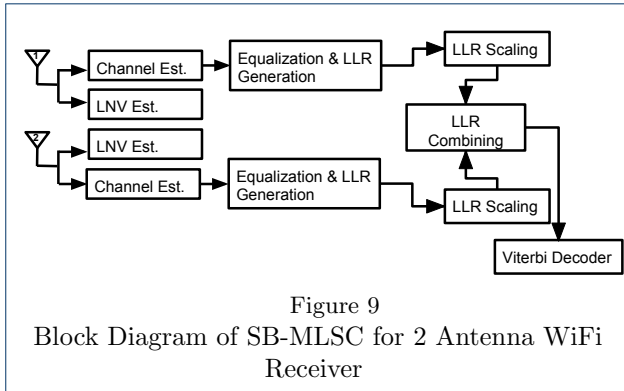
A somewhat different but simpler way to perform diversity combining, which is more popular in distributed systems, is Soft Bit Maximal Ratio Combining (SBMRC) [37][38]. In contrast to the conventional MRC which combines complex samples obtained from the different antenna branches, an SBMRC combines the LLRs from individual antenna branches. In SBMRC, the combination of bit metrics from different antenna branches, applying maximum likelihood decoding, is performed according to [37, Eq-11] as follows:

$$S_{p,l,i} \approx \frac{\min_{z \in Z_p^l} (|Y_1(i) - H_{X_1}(i)z|^2)}{\hat{\sigma}^2} + \frac{\min_{z \in Z_p^l} (|Y_2(i) - H_{X_2}(i)z|^2)}{\hat{\sigma}^2} \quad (16)$$

Where $S_{p,l,i}$ is the combined bit metrics corresponding to i -th subcarrier of l -th bit and p could be 0 or 1. Expression (16) is nothing but addition of bit metrics of l -th bit corresponding to i -th subcarrier from the two antenna branches. Hence, diversity combining can be realized by adding the LLRs from the two antenna branches, i.e.,

$$A(i, l)_{\text{SBMRC}} = A(i, l)_1 + A(i, l)_2 \quad (17)$$

where $A(i, l)_1$ and $A(i, l)_2$ are LLRs of l -th bit and i -th OFDM subcarrier corresponding to antenna branch



1 and 2 respectively. $\Lambda(i, l)_{\text{SBMRC}}$ is further fed to SDVD.

Achieving diversity combining by just adding the LLRs simplifies the way it can be implemented in SDR software. In the simulation section, we see that the performance of SBMRC is equivalent to MRC for all the experimented WiFi MCS under the same channel conditions. The reason being MRC attempts to maximize the SNR of the complex samples obtained from multiple antennas which in turn makes LLRs more strong; in contrast SBMRC tries to maximize the LLRs directly as explained in [37]. In the following, we discuss our method to implement MLSC using an easy to implement diversity combining technique SBMRC.

3.2 Method-4: Soft Bit Maximal Ratio Combiner with LLR Scaling (SB-MLSC)

In order to implement MLSC in SDR, we propose SB-MLSC which is SBMRC with LLR scaling using LNV estimates. In order to perform SB-MLSC, the LLRs from two antenna branches are added as in (17). LLR obtained after SB-MLSC, i.e., $\Lambda(i, l)_{\text{SB-MLSC}}$ can be written as:

$$\Lambda(i, l)_{\text{SB-MLSC}} = \tilde{\Lambda}(i, l)_1 + \tilde{\Lambda}(i, l)_2 \quad (18)$$

where $\tilde{\Lambda}(i, l)_m$ is the LLR corresponding l -th bit, i -th OFDM subcarrier from the m -th antenna. $\tilde{\Lambda}(i, l)_m$ is obtained after scaling according to (7) using $\hat{\sigma}_m^2(i)$, which is i -th element of LNV vector corresponding to m -th antenna. Scaling of the LLRs with their corresponding noise variances before combining them is a significant feature of SB-MLSC compared to MLSC. In MLSC the noise variances from different antennas as averaged out (14) before using them to scale the LLRs. This feature of SB-MLSC is effective when noise variance due to CCI on different receiver antennas are different. LLRs obtained using SB-MLSC are further sent to SDVD for rest of the steps of decoding. A schematic of SB-MLSC is shown in Figure 9.

Table 1: Simulation Parameters

Channel Model: Single Antenna WiFi Rx	WiFi: 11 tap frequency selective Rayleigh(RMS Delay Spread 49 ns), ZigBee: 1 tap flat fading Rayleigh
Channel Model: Dual Antenna WiFi Rx	WiFi: 11 tap frequency selective Rayleigh(RMS Delay Spread 49 ns), $\rho_X = 0.4$ ZigBee: 1 tap flat fading Rayleigh, $\rho_I = 0.1$
Noise Power	-100 dBm
WiFi PSDU	1000 bytes
ZigBee PSDU	120 bytes
Sampling Rate	WiFi 20 MHz, ZigBee oversampled to 20 MHz
WiFi Simulator	WLAN toolbox, MATLAB Release 2017b
ZigBee Simulator	LRWPAN Class, Communication Systems Toolbox, MATLAB Release 2017b

4 Simulations

To validate our methods we perform baseband Monte-Carlo simulations using standard compliant IEEE 802.11g (WiFi) and IEEE 802.15.4 (ZigBee) MATLAB packages available in release 2017b of MATLAB. We simulate the worst case scenario, i.e., as if there is no CSMA/CA, creating 100 % chance of collision. For all the experiments, we iterated until statistical reliability was achieved (in our case, until 500+ frames were erroneous).

4.1 Simulations & Results

In this section, we discuss the details of experiments, methodology and the corresponding performance metrics.

4.1.1 Experiment-1: LNV estimation and LLR scaling (LNV-SC) for single antenna WiFi receiver facing multiple narrowband interferers located on different center frequencies

In experiment-1, we simulate a single antenna WiFi-Rx capable of decoding WiFi frames using conventional method, i.e., Conv-SC as well as our method, i.e., LNV-SC simultaneously. We simulate interference between single WiFi channel and up to 4 ZigBee channels (located on different center frequencies) for WiFi MCS 0, 2, 4 and 6. Transmit Power (TXP) of ZigBee channels were fixed to -85 dBm. As a performance metric, we choose WiFi TXP required to obtain a PER of 10% [29] for LNV-SC and Conv-SC. As a reference, we also plot PER of WiFi using Conv-SC in the absence of interference.

4.1.2 Results

Results of experiment-1(Section 4.1.1) are plotted in Figure 12 (single interferer), Figure 10 (two interferers) and Figure 13 (four interferers) for MCS 0 and MCS 2. First of all, we observe that WiFi PER significantly degrades in the presence of single/multiple

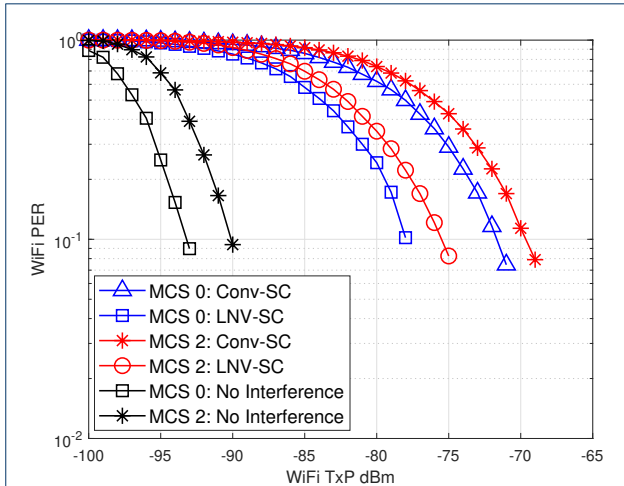


Figure 10

LNV-SC vs Conv-SC for single antenna WiFi receiver in the presence of single interferer. LNV-SC achieves more gain in SNR compared to Conv-SC for all the WiFi MCS.

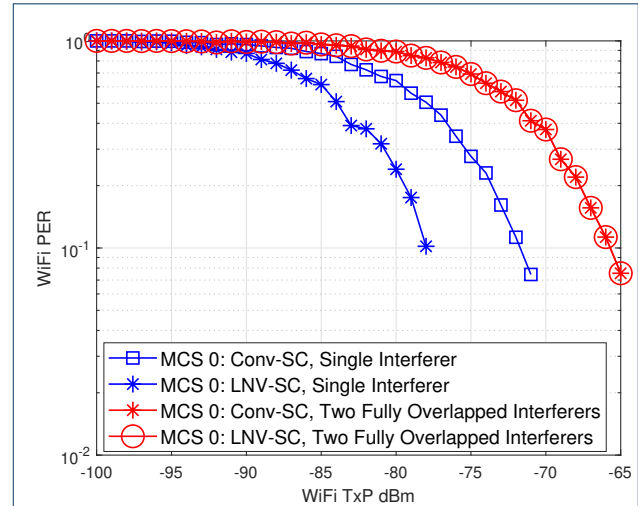


Figure 11

LNV-SC vs Conv-SC for a single antenna WiFi receiver in the presence of two fully overlapped narrowband interferers (both at -85 dBm TxP). LNV-SC fails to provide SNR gain in comparison to Conv-SC.

Table 2: SNR Gain(dB)

WiFi MCS # of Interferers	0	2	4	6
1	6.2	5.8	5.3	6.5
2	5.3	5.4	5.3	5.4
4	2	2.1	2.3	2.1

ZigBee interferers for all the WiFi MCS. Next, we observe that LNV-SC (LLR scaling with LNV estimates) achieves 10% PER mark at a lower WiFi TXP compared to the Conv-SC (conventional method) for both the WiFi MCS. Thus, our method lowers the SNR requirement in the presence of interference compared to the conventional method. The gain in SNR with our method for MCS 0, 2, 4 and 6 is summarized in Table 2

From Table 2 we observe that gain in SNR monotonically decreases as the number of interferers increase. Because, as the number of ZigBee channels increase, more WiFi subcarriers get affected which decreases the difference between noise variance estimates calculated using (2) and (4). Additionally, received ZigBee power does not decay steeply outside 2 MHz band leading to the addition of noise in more than 7 subcarriers. We also observe that the gain in SNR is more-or-less consistent throughout the WiFi MCS for a given number of interferers. The reason behind this is the fixed payload size of WiFi(1000 bytes) which we used for all the WiFi MCS during the simulations leading to an equal number of LLRs get affected for all the WiFi MCS.

4.1.3 Experiment-1.1: LNV estimation and LLR scaling (LNV-SC) for single antenna WiFi receiver facing multiple narrowband interferers located on same center frequency

In experiment-1.1, we simulate the case where a WiFi frame is affected by two fully overlapped narrowband ZigBee interferers, i.e., both the ZigBee interferers lie on the same center frequency. This is again possible due to hidden and blind terminal formation within ZigBee networks as ZigBee also uses CSMA/CA in order to capture the transmission medium. For the sake of simplicity, we took two equal powered, -85 dBm interferers.

4.1.4 Results

Results for the experiment-1.1 are plotted in Figure 11. We observe that LNV-SC fails to provide any gain over Conv-SC. The reason being excessive noise over the affected subcarriers to the extent that the LLRs are damaged beyond repair by performing LLR scaling with LNV estimates.

4.1.5 Experiment-2: Interference Detection

In experiment-2, we test our method of interference detection. As a performance metrics, we calculate the ratio of the LNV of the interfered region to that of the region without interference for fixed WiFi TXP (-80 dBm) and varying TXP of a single ZigBee channel (-100 dBm to -85 dBm). We term this ratio as *Noise Level Ratio (NLR)*. In the geometrical representation,

the level of NLR defines the height of lobes relative to the noise floor as illustrated in Figure 5. The more prominent the lobe is, the more accurate is the detection using a threshold detector.

4.1.6 Results

In Figure 14, NLR is plotted in log scale while the interference power varies from -100 dBm to -80 dBm. We observe that even at low interference TXP (-100 dBm), the NLR is 6.5 dB which is sufficient to detect the presence of interference by using a threshold detector.

4.1.7 Experiment-3: MLSC and SB-MLSC for dual antenna WiFi receiver in the presence of single narrowband interferer

In experiment-3, we first compare the performance of MRC and SBMRC under similar channel conditions in the absence of interference. Next, we compare the performance of MRC, MLSC, and SB-MLSC in the presence of single interference under similar channel conditions. Since in Experiment-1 and 2 we already showcased the effectiveness of our methods against multiple interferers, in these experiments we restrict our focus to single interferer only. We simulate dual antenna WiFi receiver capable of performing MLSC, SB-MLSC, and MRC simultaneously. During these experiments, ZigBee TXP was fixed at -85 dBm. As a performance metric, we choose WiFi TXP required to obtain a PER of 10% [29] for MRC, MLSC and SB-MLSC. Additionally, correlation ρ_X between channels of WiFi $H_{X_1}(i)$ and $H_{X_2}(i)$ is fixed to 0.4 based on the measurements shown in [39]. Since, for MRC the performance is agnostic of the correlation ρ_I between channels of ZigBee $H_{I_1}(i)$ and $H_{I_2}(i)$ [40], we fixed it to 0.1.

4.1.8 Results

We first plot the comparison result of MRC and SBMRC in ???. For the 10% PER criterion, we observe that both of them essentially perform the same for WiFi MCS 0 and 2 while SBMRC shows a slight gain at higher WiFi MCS, i.e., 4 and 6. This equivalence in performance between MRC and SBMRC encourages our choice of using SBMRC instead of MRC for achieving diversity gain as the implementation of SBMRC is simpler using SDR software packages.

Next, we plot the comparison of MRC, MLSC and SB-MLSC in Figure 15 in the presence of a single interferer. We observe that both MLSC and SB-MLSC outperform MRC for the 10% PER criterion in the presence of interference for all the WiFi MCS we experimented. The reason being that in the presence of interference, MRC does not take any measure to mitigate

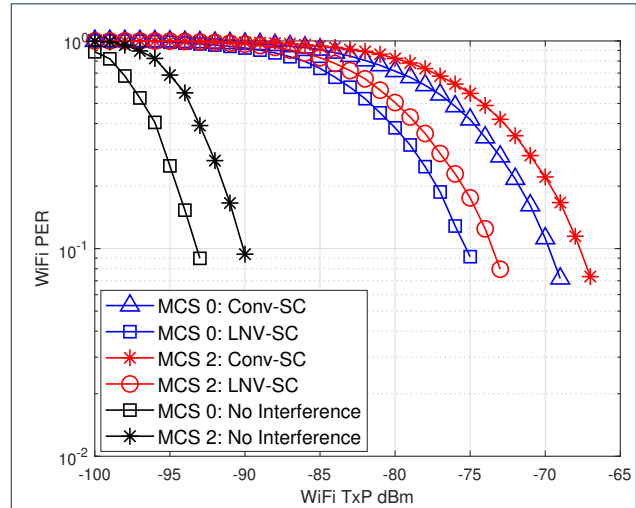


Figure 12

LNV-SC vs Conv-SC for a single antenna WiFi receiver in the presence of two narrowband interferers. LNV-SC achieves more gain in SNR compared to Conv-SC for all the WiFi MCS; although the gain decreases as the MCS increases.

it; however, both MLSC and SB-MLSC apply LNV-Sc. We also observe the equivalence in the performance of SB-MLSC and MLSC which further strengthen our choice of using SB-MLSC as an efficient alternative to MLSC which is also simpler to implement using SDR software packages.

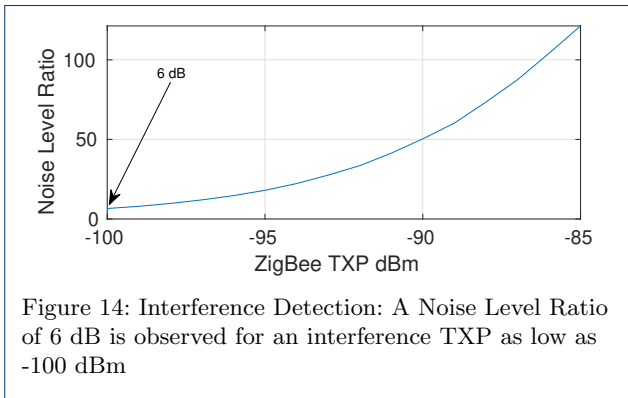
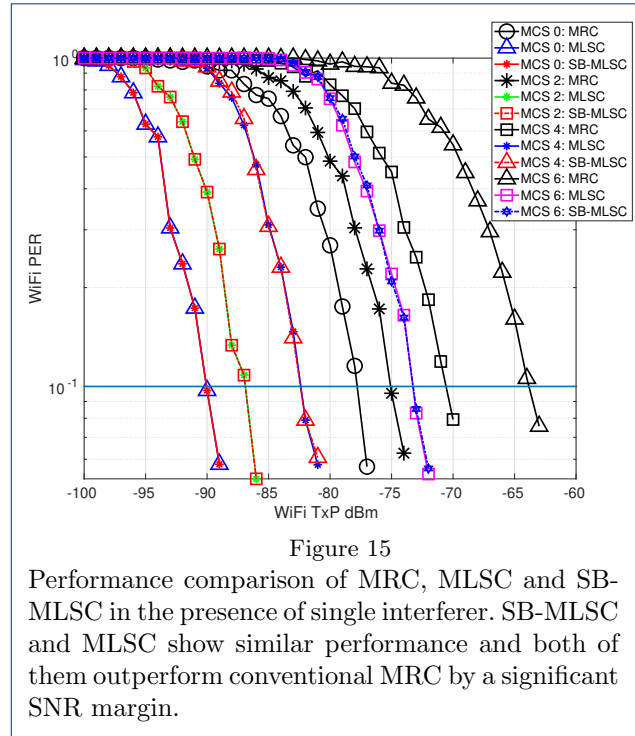
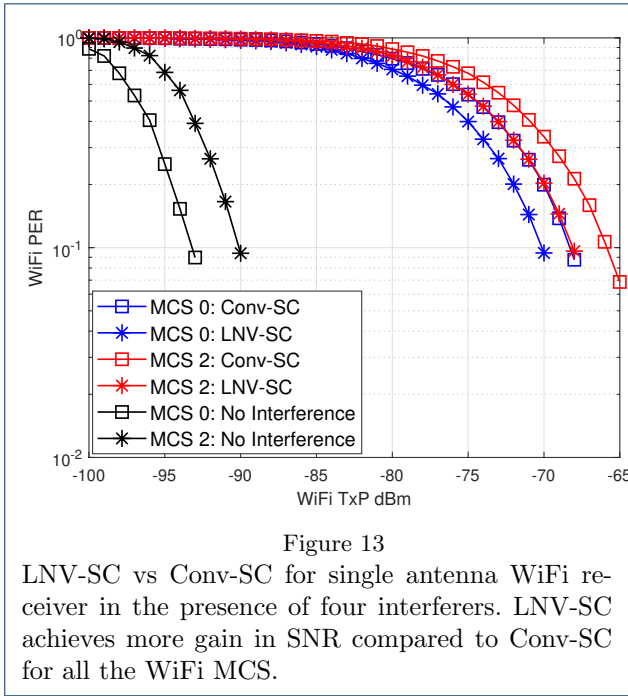
5 Software Defined Radio Implementation

For the practical applicability of our methods and real-time verification of simulation results, we prototyped our methods in Software Defined Radio (SDR). For SDR hardware, we used Universal Software Radio Peripheral [26] which is one of the most popular FPGA based hardware for wireless prototyping. On the software side, we used a combination of GNU Radio [27] and Openairinterface (OAI) [28]. In the following we discuss our SDR implementations followed by over-the-air (OTA) experiments details and test set-up.

5.1 SDR implementation of single antenna interference mitigating WiFi receiver

For this implementation, first, we developed a Soft Decision WiFi receiver using a combination of GNU Radio and Openairinterface. Both GNU Radio [36] and Openairinterface [5] contain standard compliant

^[5]Openairinterface WiFi Tx/Rx has been developed at Eurecom, France and is currently not available in public domain.



WiFi receivers. WiFi package available in GNU Radio, i.e., gr-ieee 802.11g contains Hard Decision Viterbi Decoder (HDVD) in the WiFi receiver. Hence, first, we changed the GNU Radio WiFi receiver to output LLRs as we have to perform LLR scaling for all our single antenna interference mitigating methods. In the next step, we scaled the LLRs with their corresponding LNV estimates.

Further, we integrated Soft Decision Viterbi Decoder (SDVD) available in Openairinterface WiFi receiver to decode the scaled LLRs outputted by GNU Radio. The output of the SDVD, i.e., bits are further processed using GNU Radio WiFi blocks. The code has been made open source under GPL license [41].

5.2 Implementation of SBMRC and SB-MLSC

Using our development of Soft Decision WiFi receiver, we further implemented dual antenna SBMRC and

then SB-MLSC. We added following functionalities in both SBMRC and SB-MLSC:

- Combining of the LLRs from both antenna branches happens only if
 - Frame is detected on both the antenna branches
 - SIGNAL field passes the parity check on both the antenna branches
- If any of the antenna branches fail to detect WiFi frame or the SIGNAL field parity check fails, the SBMRC starts tracking the antenna branch where both frame detection and SIGNAL parity check is successful. In other words, SBMRC operates as a selection combiner if one antenna branch fails to detect and/or decode packets.

Soft Decision WiFi receiver [41] developed by us can be easily configured to output LLRs and adding the LLRs from two antenna branches is a trivial task in GNU Radio. Hence the implementation of SBMRC and SB-MLSC is significantly simplified.

5.3 Over-the-Air Testing: Test Set-Up

The test set-up of Over-the-air (OTA) testing is shown in Figure 16. It consists of a dual-technology USRP transmitter capable of transmitting both WiFi and ZigBee frames simultaneously. Before transmission, we perform time alignment of WiFi and ZigBee frames in order to create 100% chance of a collision which replicates our simulation scenario. The frame parameters

Table 3: List of Hardware

SDR Hardware	Ettus USRP B210
SDR Software	GNU Radio Ver 3.7.1, Openairinterface, UHD 3.11
RF Cage	Ramsey STE 2200
Antenna	VERT2450 Vertical Antenna (2.4-2.5 and 4.9-5.9 GHz) Dualband
CPU	Dell Precision 5510, Gigabyte BR1X PC

of WiFi and ZigBee are the same as mentioned in Table 1; however, now the transmission happens over a physical channel. We have used RF cage for all our experiments in order to avoid interference from ambient WiFi transmissions. For the proof of concept, we have used only WiFi MCS 0 for our all the OTA experiments. Besides, GNU Radio provides tuning the transmit power gain of USRP using normalized transmit gain instead of the absolute value of gain. Hence, for all the OTA experiments, we have used normalized transmit gain values which are direct indicators of Transmit Power (TXP).

For a given TXP of WiFi and ZigBee, we repeat the same experiment 4 times. Each trial of the experiment consists of transmitting a fixed number of WiFi frames and logging the percentage of the received frames which pass the CRC test. Finally, an average is taken for plotting the results. A brief schematic of the test set-up is also shown in Figure 17 with the list of hardware used are tabulated in Table 3.

5.4 Over-the-Air Experiments

In this section, we discuss the details of experiments and the corresponding performance metrics.

5.4.1 Experiment-1: LNV Estimation and LLR Scaling (LNV-SC) in Single Antenna WiFi Receiver in the presence of One Interferer

In our first experiment, we replicate the simulation experiment as in Section 4.1.1 where a single interferer causes the interference. We used two fixed value of interferer's normalized transmit gain (0.01 and 0.05) and varied WiFi's normalized transmit gain from 0.0 till all the transmitted WiFi frames were correctly received. As a performance metrics, we chose % of packets received by each method for a given normalized transmit gain of WiFi transmitter.

5.4.2 Experiment-2: LNV Estimation and LLR Scaling (LNV-SC) in Single Antenna WiFi Receiver in the presence of Two Interferer

In this experiment, we perform the same experiment as in Section 5.4.1, but now the interference is caused by two ZigBee interferer. We implemented two ZigBee interferers in the baseband with a separation of 5 MHz between the center frequencies and then transmitted

them using a single antenna. We used two fixed value of interferer's normalized transmit gain (0.01 and 0.05) and varied WiFi's normalized transmit gain from 0.0 till all the transmitted WiFi frames were correctly received. As a performance metrics, we chose % of packets received by each method for a given normalized transmit gain of WiFi transmitter.

5.4.3 Experiment-3: SB-MLSC for two antenna WiFi Receiver in the presence of One Interferer

In this experiment, we attempt to replicate the simulation experiment as in Section 4.1.7. OTA testing of SB-MLSC was tricky because it has to be done inside an RF cage where multi-paths are not possible due to thick absorbent layer inside it. Also, inside the RF cage where antennas are placed nearby, the strength of interference on all the antenna branches are nearly equal, and hence the effect is the same. The idea behind exploiting multi-paths is that once interference arrives via different paths, its strength is different on the different antennas of the receiver. CCI on WiFi packets obtained from any of the receive antenna branches depends on the interference power on that antenna branch. Knowing that the ultimate effect due to CCI on WiFi packet is CRC fail, we decided to improve our test methodology by manually emulating the CCI effect. We decreased the strength of WiFi signal on one of the antenna branches by partially/fully covering one of the receive antenna branches using aluminum foils. As the previous two experiments already showcased the effectiveness of our interference mitigation methods, we limit our scope in this experiment to the verification of operational and tracking capabilities of SB-MLSC. We analyzed the following three cases during this experiment.

- **Case-1:** Partially covering one of the receive antenna branches: This reduces the WiFi signal strength on that antenna branch.
- **Case-2:** Fully covering one of the receive antenna branches with aluminum foil: This nulls the WiFi signal strength on that antenna branch.
- **Case-3:** Placing scrambled aluminum foils inside the RF cage: This was done in an attempt to emulate multi-path reflections inside the RF cage.

5.5 OTA Results and Discussion

5.5.1 Experiment-1

The bar chart for this experiment is shown in Figure-18. First of all, we observe that due to ZigBee interference the % of received WiFi packets (which pass the CRC test) severely degrades. For example, the bars corresponding to LNV-SC and Conv-SC lags behind the blue bars (W/o means without). This result agrees with our simulation results. We observe this

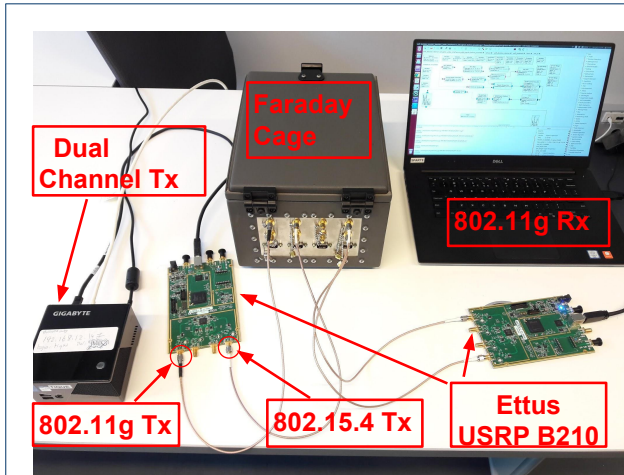


Figure 16: Over-the-air test set-Up: USRP B210, RF Cage and General Purpose CPU

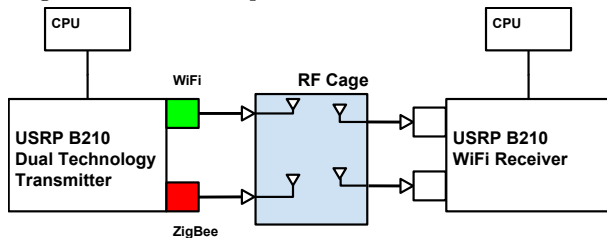


Figure 17: Over-the-air Test Schematic corresponding to Figure 16

degradation for both ZigBee normalized transmit gain of 0.01 and 0.05. Next, we observe that for a given % of received WiFi packets, performing LLR scaling with LNV (Proposed method LNV-SC) significantly reduces the transmit power requirement compared to the conventional method (Conv-SC). For example, for interferer's normalized transmit gain of 0.05, the green bars lag behind the violet bars. As expected, as the normalized transmit gain of WiFi is increased, WiFi dominates over interference, and both the methods show the same performance.

5.5.2 Experiment-2

The bar chart for this test is shown in Figure-19. Similar to the previous experiment-1, we observe that due to ZigBee interference the % of received WiFi packets (which pass the CRC test) severely decreases. However, the performance degradation is more compared to the single interferer case. For example, the orange bars in Figure-19 lag behind the orange bars in Figure-18. This also agrees with our simulation results. We observe this for both the ZigBee normalized transmit gain of 0.01 and 0.05. Next, just like experiment-1, we observe that for a given % of received WiFi packets,

performing LLR scaling with LNV (LNV-SC) reduces the transmit power requirement significantly compared to the conventional method (Conv-SC). For example, for interferer's normalized transmit gain of 0.05, the green bars lag behind the violet bars.

5.5.3 Experiment-3

We present three different sets of results corresponding to the three cases discussed in Section 5.4.3.

- 1 The results corresponding to the case-1 are plotted in Figure-20. We performed 3 trials of the experiment (with different interference TXP) wherein each we partially covered the receive antenna branch 2 with aluminum foil which resulted in SB-MLSC tracking the branch 1 which was stronger.
- 2 The results corresponding to the case-2 are plotted in Figure-21. We performed 3 trials of the experiment (with different interference TXP) where we completely covered the receive antenna branch-1 with aluminum foil which effectively stopped branch-1 from receiving any WiFi frame. This resulted in SB-MLSC receiving the same number of WiFi packets as antenna branch-2, i.e., SB-MLSC again tracked the stronger branch and behaved as a selection combiner.
- 3 The results corresponding to the case-3 are plotted in Figure-22. We placed scrambled aluminum foils inside the RF cage to emulate multi-path reflections. We performed 3 trials of the experiment where we changed the positions of aluminum foils inside the RF cage. We indeed observe diversity gain for several placement scenarios of the scrambled aluminum foil although the gain was marginal.

Results corresponding to all the three cases of Experiment - 3 indicate the proper operation and tracking capability of SB-MLSC.

6 Conclusions

In this work, we have addressed the co-channel interference faced by wideband OFDM based WiFi due to single/multiple narrowband ZigBee interferers in the 2.4 GHz ISM Band. First, we describe single and multi-antenna interference mitigating receiver architecture for WiFi which is based on the localized estimation of excess noise caused by single and multiple narrowband co-channel interferers. We also proposed a simple yet effective method for immediate detection of multiple narrowband interferers which is a byproduct of our single antenna method. Next, we extended our method for multi-antenna WiFi receivers and proposed MLSC which is Maximal Ratio Combiner with LLR Scaling. MLSC apart from interference mitigation also

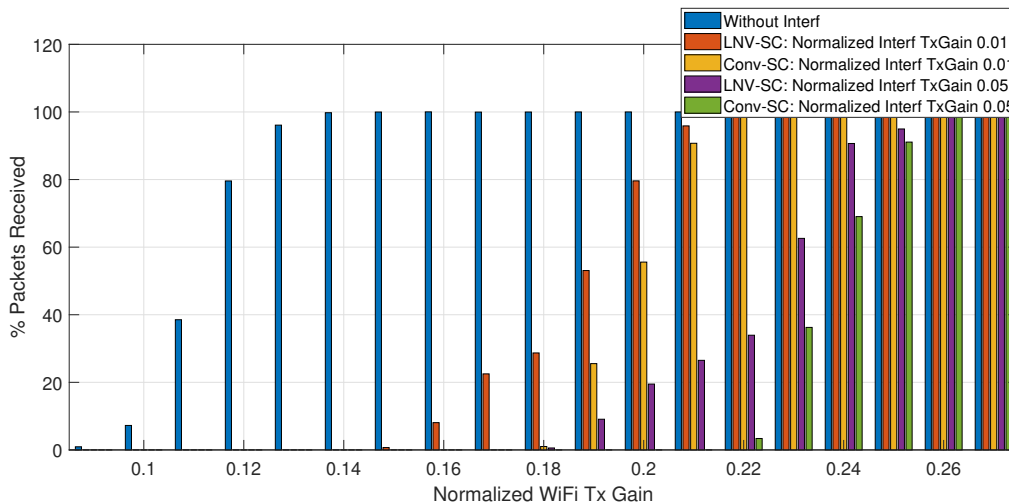


Figure-18: LNV-SC (proposed method) in the single interferer case leads to more WiFi frames passing CRC test compared to Conv-SC (conventional method) at a lower WiFi TXP. This is observed for both the experimented interferer TXP

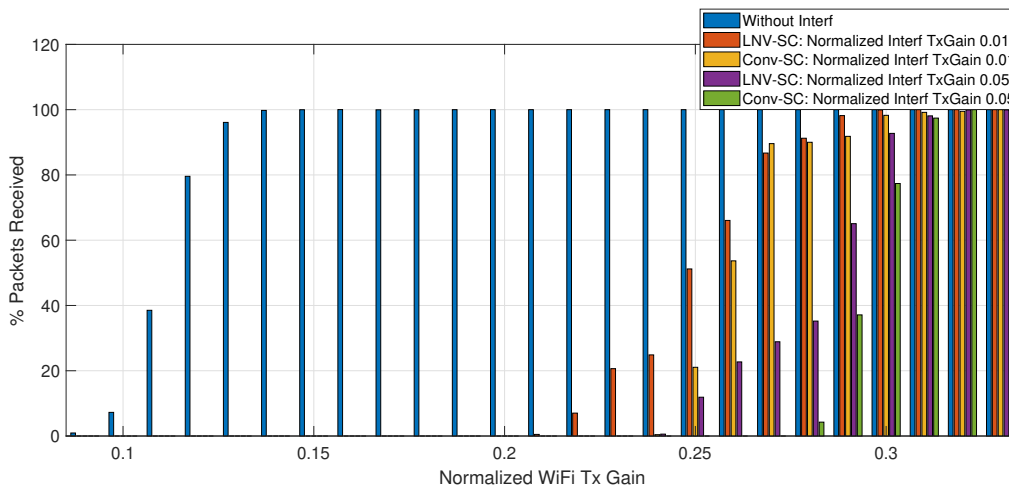
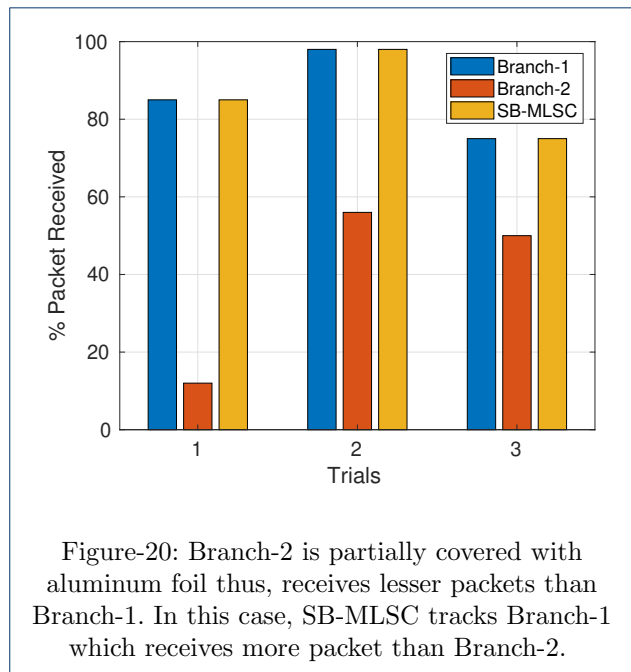


Figure-19: LNV-SC (proposed method) in the two interferer case also leads to more WiFi frames passing CRC test compared to Conv-SC (conventional method) at a lower WiFi TXP. This is observed for both the experimented interferer TXP

provides diversity gain. For both our methods – single and multi-antenna – simulation results show significant SNR gain compared to conventional methods.

Further, we proposed SB-MLSC which is Soft Bit Maximal Ratio Combiner with LLR scaling. In simulations, SB-MLSC performs equivalently to MLSC in terms of diversity gain and interference mitigation; however, it is easy to implement. Finally, we implemented all our methods using USRP SDR and verified their functionality by performing over-the-air (OTA) tests using standard compliant WiFi and Zig-

Bee frames. Results of OTA tests fall in agreement with our simulation results indicating the practical applicability of our methods. Our methods are applicable to all the wireless standards which are based on OFDM and face narrowband co-channel interference. Finally, all the methods we propose require modifications only on the receiver side, and hence they can be integrated into existing infrastructure with minimal modifications.



7 Declarations

7.1 Abbreviations

LNV: Local Noise Variance; SIC: Successive Interference Cancellation; MLSC: Maximal Ratio Combiner with LLR Scaling; SB-MLSC: Soft Bit Maximal Ratio Combining with LLR Scaling; SBMRC: Soft Bit Maximal Ratio Combining; TXP: Transmit Power; CCI: Co-Channel Interference; ISM: Industrial Scientific and Medical; LLR: Log Likelihood Ratios; CSMA/CA: Carrier Sense Multiple Access with Collision Avoidance; OTA: Over the Air; SDR: Software Defined Radio; M2M: Machine to Machine; LNV-SC: Local Noise Variance LLR Scaling; Conv-SC: Conventional Scaling;

7.2 Availability of data and materials

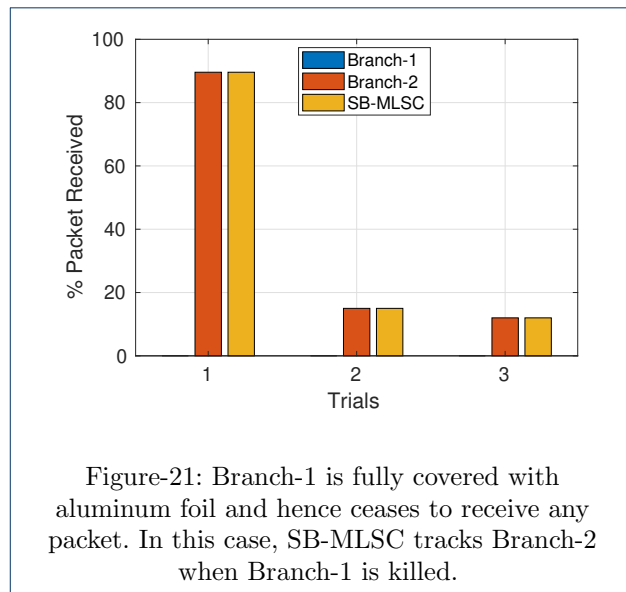
Data sharing is not applicable to this article as no datasets were generated or analyzed during the current study.

7.3 Authors' contributions

SK carried out the theoretical studies, hardware implementation and drafting the manuscript. FK participated in the Software Defined Radio implementation of the proposed methods. All authors read and approved the final manuscript.

7.4 Competing interests

The authors declare that they have no competing interests.



7.5 Funding

This work has received funding from Siemens AG Corporate Technology, Munich, Germany.

7.6 Acknowledgements

We are thankful to Alejandro Ramirez and Bernhard Kloiber from Siemens AG Corporate Technology, Munich, Germany for their valuable feedback and review of the manuscript.

7.7 Figure Titles and Legend

Figure-1: WiFi-ZigBee frequency allocation in 2.4GHz ISM band(Top) and overlap between single WiFi and single ZigBee channel (Bottom)

Figure-2: PER of single antenna WiFi receiver in the presence and absence of single antenna ZigBee transmitter(transmit power -85 dBm). For all WiFi MCS, we observe severe PER degradation.

Figure-3: WiFi Frame Structure: LTS-1 and LTS-2 are used for channel and noise variance estimation.

Figure-4: Set of interfered and interference-free WiFi Subcarriers facing interference by 4 Co-Channel ZigBee Interferers

Figure-5: LNV estimates corresponding to 4 ZigBee Interferers. Distinguish lobes appear at ZigBee center frequencies due to LNV estimation.

Figure-6: Flow Chart of Interference Detection and LLR Scaling. LLR scaling using LNV (LNV-SC) to be performed only during interference.

Figure-7: Signal Model: Single Antenna WiFi Transmitter, Single Antenna ZigBee Interferer and Two Antenna WiFi receiver

Figure-8: Schematic of Proposed MLSC for 2 Antenna WiFi Receiver

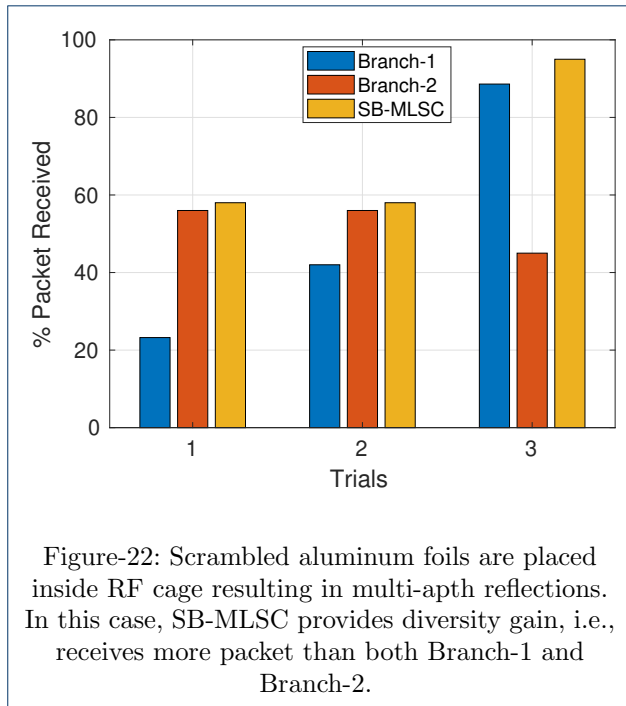


Figure-9: Block Diagram of SB-MLSC for 2 Antenna WiFi Receiver

Figure-10: LNV-SC vs Conv-SC for single antenna WiFi receiver in the presence of a single interferer. LNV-SC achieves more gain in SNR compared to Conv-SC for all the WiFi MCS.

Figure-11: LNV-SC vs Conv-SC for single antenna WiFi receiver in the presence of two fully overlapped narrowband interferers (both at -85 dBm TxP). LNV-SC fails to provide SNR gain in comparison to Conv-SC.

Figure-12: LNV-SC vs Conv-SC for single antenna WiFi receiver in the presence of two interferers. LNV-SC achieves more gain in SNR compared to Conv-SC for all the WiFi MCS.

Figure-13: LNV-SC vs Conv-SC for single antenna WiFi receiver in the presence of four interferers. LNV-SC achieves more gain in SNR compared to Conv-SC for all the WiFi MCS.

Figure-14: Interference Detection: A Noise Level Ratio of 6 dB is observed for an interference TXP as low as -100 dBm

Figure-15: Performance comparison of MRC, MLSC and SB-MLSC in the presence of single interferer. SB-MLSC and MLSC show similar performance and both of them outperform conventional MRC by a significant SNR margin.

Figure-16: Over-the-air test set-Up: USRP B210, RF Cage and General Purpose CPU

Figure-17: Over-the-air Test Schematic corresponding to Figure 16

Figure-18: LNV-SC (proposed method) in the single interferer case leads to more WiFi frames passing CRC test compared to Conv-SC (conventional method) at a lower WiFi TXP. This is observed for both the experimented interferer TXP.

Figure-19: LNV-SC (proposed method) in the two interferer case also leads to more WiFi frames passing CRC test compared to Conv-SC (conventional method) at a lower WiFi TXP. This is observed for both the experimented interferer TXP.

Figure-20: Branch-2 is partially covered with aluminum foil thus, receives lesser packets than Branch-1. In this case, SB-MLSC tracks Branch-1 which receives more packet than Branch-2.

Figure-21: Branch-1 is fully covered with aluminum foil and hence ceases to receive any packet. In this case, SB-MLSC tracks Branch-2 when Branch-1 is killed.

Figure-22: Scrambled aluminum foils are placed inside RF cage resulting in multi-apth reflections. In this case, SB-MLSC provides diversity gain, i.e., receives more packet than both Branch-1 and Branch-2.

Author details

¹Communication Systems, Eurecom, Sophia Antipolis, Biot, France.

²Siemens AG Corporate Technology, Munich, Germany.

References

1. Yubo, Y., Panlong, Y., Xiangyang, L., Yue, T., Lan, Z., Lizhao, Y.: Zimo: Building cross-technology mimo to harmonize ZIGBEE smog with WIFI flash without intervention. In: Proceedings of the 19th Annual International Conference on Mobile Computing & Networking, pp. 465–476 (2013). ACM
2. Zhao, Z., Wu, X., Zhang, X., Zhao, J., Li, X.-Y.: ZIGBEE vs WIFI: Understanding issues and measuring performances of their coexistence. In: Performance Computing and Communications Conference (IPCCC), 2014 IEEE International, pp. 1–8 (2014). IEEE
3. Yan, Y., Yang, P., Li, X.-Y., Zhang, Y., Lu, J., You, L., Wang, J., Han, J., Xiong, Y.: Wizbee: Wise ZIGBEE coexistence via interference cancellation with single antenna. IEEE Transactions on Mobile Computing **14**(12), 2590–2603 (2015)
4. Sheu, S.-T., Shih, Y.-Y., Lee, W.-T.: Cdma/cf protocol for ieee 802.15. 4 wpans. IEEE Transactions on vehicular technology **58**(3), 1501–1516 (2008)
5. Tseng, Y.-C., Ni, S.-Y., Shih, E.-Y.: Adaptive approaches to relieving broadcast storms in a wireless multihop mobile ad hoc network. IEEE transactions on computers **52**(5), 545–557 (2003)
6. Liang, C.-J.M., Priyantha, N.B., Liu, J., Terzis, A.: Surviving WIFI interference in low power ZIGBEE networks. In: Proceedings of the 8th ACM Conference on Embedded Networked Sensor Systems, pp. 309–322 (2010). ACM
7. Liang, C.-J.M., Priyantha, N.B., Liu, J., Terzis, A.: Surviving wi-fi interference in low power ZIGBEE networks. In: Proceedings of the 8th ACM Conference on Embedded Networked Sensor Systems, pp. 309–322 (2010). ACM
8. Terzis, A., et al.: Minimising the effect of WIFI interference in 802.15. 4 wireless sensor networks. International Journal of Sensor Networks **3**(1), 43–54 (2007)
9. Xu, R., Shi, G., Luo, J., Zhao, Z., Shu, Y.: Muzi: Multi-channel ZIGBEE networks for avoiding WIFI interference. In: Internet of Things (iThings/CPSCoM), 2011 International Conference on and 4th International Conference on Cyber, Physical and Social Computing, pp. 323–329 (2011). IEEE

10. Kumar, S., Kaltenberger, F., Ramirez, A., Kloiber, B.: A robust decoding method for OFDM systems under multiple co-channel narrowband interferers. In: 2018 European Conference on Networks and Communications (EuCNC), pp. 368–372 (2018). IEEE
11. Kumar, S., Kaltenberger, F., Ramirez, A., Kloiber, B.: Robust OFDM diversity receiver under co-channel narrowband interference. In: WIMOB 2018, 14th International Conference on Wireless and Mobile Computing, Networking and Communications, 15-17 October 2018, Limassol, Cyprus, Limassol, CHYPRE (2018). <http://www.eurecom.fr/publication/5654>
12. Miridakis, N.I., Vergados, D.D.: A survey on the successive interference cancellation performance for single-antenna and multiple-antenna OFDM systems. *IEEE Communications Surveys & Tutorials* **15**(1), 312–335 (2013)
13. Sen, S., Santhapuri, N., Choudhury, R.R., Nelakuditi, S.: Successive interference cancellation: Carving out mac layer opportunities. *IEEE Transactions on Mobile Computing* **12**(2), 346–357 (2013)
14. Halperin, D., Anderson, T., Wetherall, D.: Taking the sting out of carrier sense: interference cancellation for wireless lans. In: Proceedings of the 14th ACM International Conference on Mobile Computing and Networking, pp. 339–350 (2008). ACM
15. Zhang, X., Shin, K.G.: Cooperative carrier signaling: Harmonizing coexisting wpan and wlan devices. *IEEE/ACM Transactions on Networking (TON)* **21**(2), 426–439 (2013)
16. Pelechrinis, K., Broustis, I., Krishnamurthy, S.V., Gkantsidis, C.: Ares: an anti-jamming reinforcement system for 802.11 networks. In: Proceedings of the 5th International Conference on Emerging Networking Experiments and Technologies, pp. 181–192 (2009). ACM
17. Tan, K., Liu, H., Fang, J., Wang, W., Zhang, J., Chen, M., Voelker, G.M.: Sam: enabling practical spatial multiple access in wireless lan. In: Proceedings of the 15th Annual International Conference on Mobile Computing and Networking, pp. 49–60 (2009). ACM
18. Gollakota, S., Perli, S.D., Katabi, D.: Interference alignment and cancellation. In: ACM SIGCOMM Computer Communication Review, vol. 39, pp. 159–170 (2009). ACM
19. Seo, B.-S., Choi, S.-G., Cha, J.-S.: Maximum ratio combining for OFDM systems with cochannel interference. *IEEE Transactions on Consumer Electronics* **52**(1), 87–91 (2006)
20. Ahmed, R., Eitel, B., Speidel, J.: Enhanced maximum ratio combining for mobile dvb-t reception in doubly selective channels. In: Vehicular Technology Conference (VTC Spring), 2015 IEEE 81st, pp. 1–5 (2015). IEEE
21. Lee, W.-C., Cho, C.-H., Kwak, J.-H., Park, M.-Y., Kang, K.-J.: Viterbi decoding method using channel state information in COFDM system. In: Consumer Electronics, 1999. ICCE. International Conference On, pp. 66–67 (1999). IEEE
22. Gollakota, S., Adib, F., Katabi, D., Seshan, S.: Clearing the rf smog: making 802.11 n robust to cross-technology interference. In: ACM SIGCOMM Computer Communication Review, vol. 41, pp. 170–181 (2011). ACM
23. Winters, J.H.: Optimum combining in digital mobile radio with cochannel interference. *IEEE Transactions on Vehicular Technology* **33**(3), 144–155 (1984)
24. Croce, D., Garlisi, D., Giuliano, F., Tinnirello, I.: Learning from errors: Detecting ZIGBEE interference in WIFI networks. In: Ad Hoc Networking Workshop (MED-HOC-NET), 2014 13th Annual Mediterranean, pp. 158–163 (2014). IEEE
25. Croce, D., Gallo, P., Garlisi, D., Giuliano, F., Mangione, S., Tinnirello, I.: Errorsense: Characterizing WIFI error patterns for detecting ZIGBEE interference. In: Wireless Communications and Mobile Computing Conference (IWCMC), 2014 International, pp. 447–452 (2014). IEEE
26. Agency, W.L.I.: Ettus Research, an NI Brand. <https://www.ettus.com/> Accessed 2018-11-16
27. Radio, G.: GNU Radio. <https://www.gnuradio.org/> Accessed 2018-11-16
28. Kaltenberger, F., Jiang, X., Knopp, R.: From massive MIMO to C-RAN: the OpenAirInterface 5G testbed. In: ASILOMAR 2017, Asilomar Conference on Signals, Systems, and Computers, October 29th–November 1st 2017, Pacific Grove, CA, USA, Pacific Grove, ÉTATS-UNIS (2017). doi:10.1109/ACSSC.2017.8335413. <http://www.eurecom.fr/publication/5413>
29. IEEE Computer Society LAN MAN Standards Committee and others: Wireless lan medium access control (mac) and physical layer (phy) specifications. ANSI/IEEE Std. 802.11-1999 (1999)
30. Ren, G., Zhang, H., Chang, Y.: Snr estimation algorithm based on the preamble of OFDM systems in frequency selective channels. *IEEE Transactions on Communications* **57**(8) (2009)
31. Viterbi, A.J.: An intuitive justification and a simplified implementation of the map decoder for convolutional codes. *IEEE Journal on Selected Areas in Communications* **16**(2), 260–264 (1998)
32. Sandell, M., Tosato, F., Ismail, A.: Low complexity max-log llr computation for nonuniform pam constellations. *IEEE Communications Letters* **20**(5), 838–841 (2016)
33. Azimi-Sadjadi, B., Sexton, D., Liu, P., Mahony, M.: Interference effect on ieee 802.15. 4 performance. In: Proceedings of 3rd International Conference on Networked Sensing Systems (INNS), Chicago, IL (2006)
34. Goldsmith, A.: *Wireless communications* (2005)
35. Stüber, G.L.: *Principles of mobile communication 2* (1996)
36. Bloessl, B.: IEEE 802.11 A/g/p Transceiver. <https://github.com/bastibl/gr-ieee802-11>
37. Ouyang, X., Ghosh, M., Meehan, J.P.: Optimal antenna diversity combining for ieee 802.11 a system. *IEEE Transactions on Consumer Electronics* **48**(3), 738–742 (2002)
38. Sediq, A.B., Yanikomeroğlu, H.: Performance analysis of soft-bit maximal ratio combining in cooperative relay networks. *IEEE Transactions on Wireless Communications* **8**(10) (2009)
39. Kafle, P.L., Intarapanich, A., Sesay, A.B., McRory, J., Davies, R.J.: Spatial correlation and capacity measurements for wideband mimo channels in indoor office environment. *IEEE Transactions on wireless communications* **7**(5) (2008)
40. Cui, J., Falconer, D.D., Sheikh, A.U.: Performance evaluation of optimum combining and maximal ratio combining in the presence of co-channel interference and channel correlation for wireless communication systems. *Mobile Networks and Applications* **2**(4), 315–324 (1997)
41. Kumar, S.: Soft Decision Viterbi Decoder for WIFI. <https://github.com/sumitstop/SDVD-WiFi>